Small-angle scattering features of lyotropic smectics A

F. Nallet, D. Roux, S.T. Milner

J. Phys. France **51** (1990) 2333-2346 15 OCTOBRE **1990,** PAGE 2333

Classification
Physics Abstracts
61.30E — 82.70D

Small-angle scattering features of lyotropic smectics A

F. Nallet ([1]), D. Roux ([1]) and S. T. Milner ([2])

([1]) CNRS, Centre de recherche Paul-Pascal, avenue du Docteur-Schweitzer, F-33600 Pessac, France
([2]) Corporate Research Science Laboratories, Exxon Research and Engineering Company, Annandale, NJ 08801, USA

(*Received 6 April 1990, accepted in final form 13 June 1990*)

Résumé. — La phase smectique A lyotrope diluée a été étudiée par une expérience de diffusion de neutrons aux petits angles réalisée sur des échantillons orientés. Le facteur de structure d'un smectique A binaire est établi théoriquement en considérant explicitement le couplage anisotrope entre les fluctuations de concentration et celles de déplacement des couches. La diffusion aux petits angles ainsi que d'autres caractéristiques remarquables des spectres, de même que leur devenir au cours de la dilution, sont prévus. L'accent est mis sur les différences entre phases lamellaires diluées suivant que leur stabilité a pour cause l'interaction électrostatique non amoindrie ou l'interaction stérique d'ondulation. La théorie fournit un cadre cohérent pour l'interprétation de l'expérience.

Abstract. — Small-angle neutron scattering experiments on dilute lyotropic smectics A have been performed on oriented samples. The structure factor of a two-component smectic A is derived theoretically, taking explicitly into account the anisotropic coupling between concentration and layer displacement fluctuations. The anisotropic small-angle signal and other characteristic features of the spectra, and their evolutions with dilution, are predicted. The differences between electrostatically and sterically stabilized dilute lamellar phases are emphasized. Experiments are consistently described by the theory.

Introduction.

The smectic A phase of *multicomponent* surfactant/solvent systems sometimes displays a remarkable feature : it exists over a wide range of surfactant concentration (surfactant volume fractions from a few ten % down to less than one %), the smectic repeat distance d varying continuously upon addition of a solvent from molecular sizes up to very large values (repeat distances about 1 μm have been reported [1-5]). In the dilute range, a *colloidal* smectic phase is obtained. This dilute phase is interesting because its macroscopic — thermodynamic and hydrodynamic — properties can presumably be described in universal terms, without any explicit reference to detailed molecular characteristics. It is pictured as a stack of *membranes* — the surfactant bilayers, with typical thicknesses δ about 30 Å —

interacting by means of short range (hydration [6], screened electrostatic) or long range (Van der Waals, electrostatic) forces. The membranes themselves are characterized, in terms of the Helfrich elastic energy density [7], by their bending modulus κ. The particular case when κ becomes comparable to the thermal energy $k_B T$ deserves special interest, since thermally excited undulation fluctuations of each membrane are now striving for large amplitudes, but are hindered by the presence of neighbouring membranes. The resulting loss of conformational entropy leads to an effective *long range repulsion* [8], which overwhelms the Van der Waals attraction at large intermembrane distances and which accounts for the stability at high dilution of the smectic phase in non-electrostatic systems. The relevance of such a theoretical scheme to describing macroscopic properties of colloidal smectics [8-10] is provided, for example, by static [11-13] or dynamic [14-15] scattering measurements of smectic elastic constants or by direct measurements of intermembrane forces [16].

Static X-ray or neutron scattering experiments on colloidal smectics were at first [11, 17] mainly concerned with the study of the precise shape of the quasi-Bragg peak associated with the quasi-long range one-dimensional translational order characteristic of *any* smectic A phase. It is indeed well-known that this shape is controlled by the elastic constants of the smectic phase [18-20]. However, in addition to a quasi-Bragg peak, the recorded spectra display an « unexpected » small-angle scattering that many become so strong as to thoroughly overwhelm the quasi-Bragg singularity [11]. The small-angle signal was first specifically studied by Porte and coworkers : working on cylindrically oriented samples, they showed that it was anisotropic [21]. They ascribed its origin to surfactant concentration fluctuations linked to membrane undulations, and, by means of a numerical evaluation of correlation functions, predicted an universal line shape for sterically stabilized dilute lyotropic smectics [22]. It is our aim in this paper to deepen their study : in the first part, we present our results of a small-angle neutron scattering study of various sterically or electrostatically stabilized lamellar phases, performed on planar oriented samples ; the second part is devoted to the analytic computation of the correlation functions of interest, based upon a very general harmonic description of a two-component smectic A phase. Our model rests on the concentration fluctuation mechanism originally proposed by Porte and coworkers [22] but in contrast with them we find a non-universal line shape. In the third part, we interpret our data with the model and extract estimates of various elastic parameters.

Part 1.

In order to observe conveniently the small-angle spectrum of oriented samples, neutron scattering is the most suitable technique : oriented samples can be got in large volume cells ; the use of deuterated water enhances the contrast ; 2D detectors are routinely available for quantitative analyses ; there is no need of high resolution to record the small-angle signal. The small-angle neutron scattering experiments have been performed on the neutron line PAXY equipped with a two-dimensional detector at Laboratoire Léon-Brillouin, CEN-Saclay, France. For most of our experiments, the neutron wavelength was $\lambda = 8$ Å with a sample-to-counter distance $L = 6.786$ m. The sample cells are analogous to the ones described by Charvolin and Hendrikx [23] : about 20 rectangular (30×5 mm^2, thickness 180 μm) quartz plates are held parallel, roughly 200 μm apart, by two glass-charged Teflon combs within $10 \times 10 \times 50$ mm^3 quartz cells. The cells are filled by capillarity, then mildly centrifugated to get rid of remaining air bubbles, plugged with a Teflon cap and sealed with glue. The orientation of the surfactant layers parallel to the quartz plates is achieved by means of a thermal cycle : the samples are heated up to the isotropic phase, let to stand at that temperature (60-80 °C) for a few hours, then slowly cooled down to room temperature (at

about – 0.5 °C /min). In order to improve tightness, the cells are enclosed in small bottles during the thermal cycle. The scattering experiments are performed with the long sides of the rectangular quartz plates perpendicular, and the small sides either parallel (planar orientation) or perpendicular (homeotropic orientation) to the neutron beam. In the planar configuration, the spanned reciprocal space is :

$$8 \times 10^{-2}\ \mathrm{nm}^{-1} \leqslant q_z \leqslant 8 \times 10^{-1}\ \mathrm{nm}^{-1}, \quad , -6 \times 10^{-1}\ \mathrm{nm}^{-1} \leqslant q_\perp \leqslant 6 \times 10^{-1}\ \mathrm{nm}^{-1},$$

where the z-direction is along the normal to the smectic layers.

The studied samples belong to three series : « oil dilution », when the sodium dodecylsulphate (SDS)-pentanol-water bilayer is diluted by addition of a dodecane-pentanol solvent ; « brine dilution » (SDS-pentanol membrane, water-NaCl solvent) ; « water dilution » (two groups : SDS-hexanol membrane, water ; or didodecyldimethylammonium bromide (DDAB) membrane, water). The only deuterated species is water.

Perspective views of the 2D scattering profiles obtained in the planar configuration for the SDS series are displayed in figures 1-3. The intensity is mainly scattered along the q_z-axis, with noticeable Bragg peaks for the less dilute samples. The anisotropy of the figures implies that the samples are, at least partially, oriented : a powder would have given isotropic rings instead of Bragg peaks, for instance. The quality of the orientation can be checked more stringently on *homeotropic* spectra : perfectly oriented samples should then display an isotropic scattering without Bragg peak, whereas we still get spectra qualitatively similar to the ones observed with the planar orientation, though at much lower intensities. This means that the remaining disoriented parts of our samples are not powder-like but still appear as

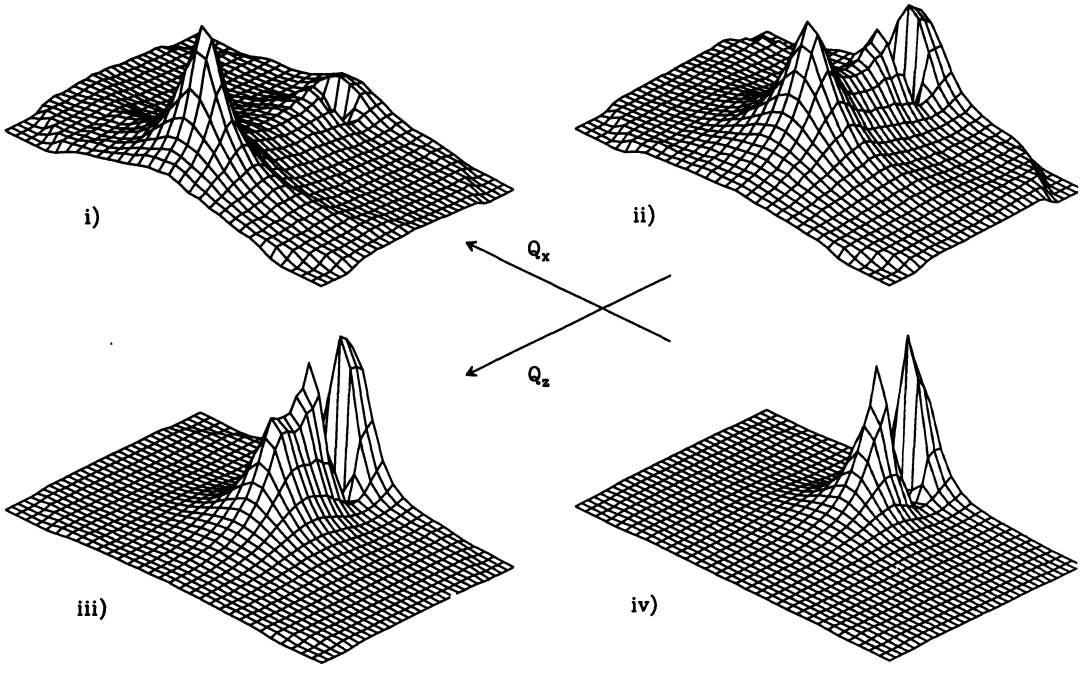

Fig. 1. — Two-dimensional scattering profiles of four oil-diluted SDS samples. The smectic repeat distances are, respectively : i) d = 10.3 nm ; ii) d = 15.0 nm ; iii) d = 23.3 nm ; iv) d = 34.9 nm. The well in the profile is the shadow of the beam-trap.

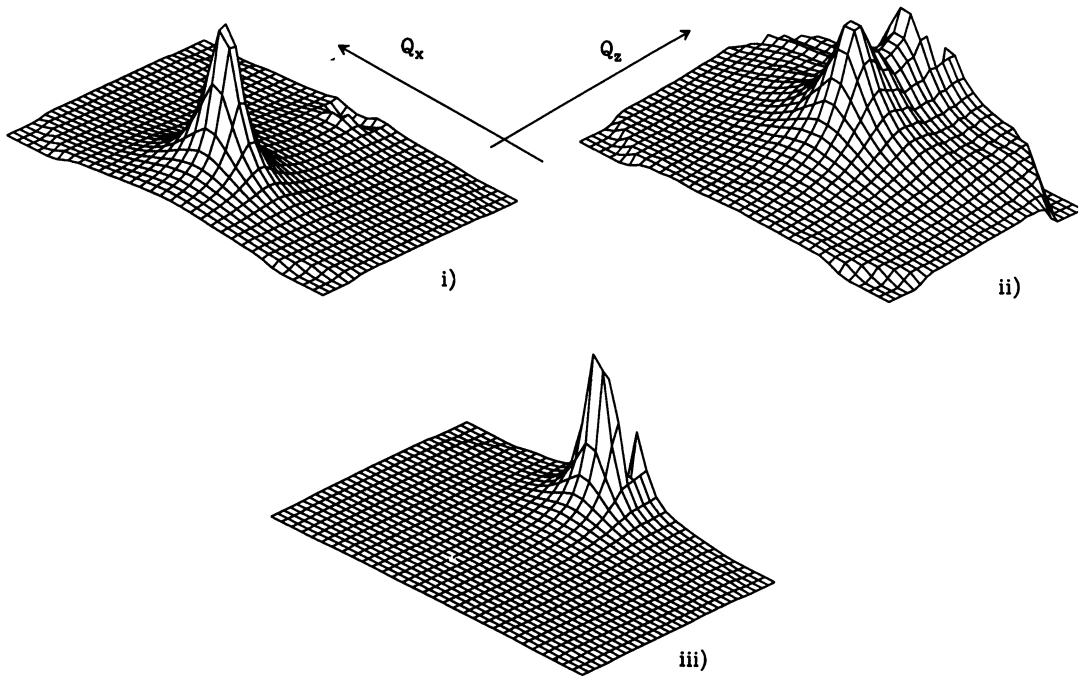

Fig. 2. — Two-dimensional scattering profiles of three brine-diluted SDS samples. The smectic repeat distances are, respectively : i) $d = 13.4$ nm ; ii) $d = 24.2$ nm ; iii) (extrapolated value) $d = 105$ nm. Compare graphs i) and ii) here with the corresponding dilutions in figure 1, i.e. with graphs ii) and iii).

oriented domains. They have a low volume fraction : the Bragg peak intensity is at least 10 times smaller for the homeotropic orientation as compared to the planar one. On the other hand, it was not possible to get oriented DDAB samples : the 2D profiles for both planar and homeotropic orientations of the cell display *isotropic* Bragg rings. The 1D spectra (resulting from the isotropic averaging over the 2D multidetector) are displayed in figure 4.

The scattering profiles for the oil or brine dilutions differ qualitatively in two respects from those yielded by the water-diluted samples : i) the former only display a first order Bragg peak (in the low surfactant content limit), whereas two or three peaks are observed with the latter, even at high dilution ; ii) an *anisotropic* small-angle scattering, rapidly increasing, as swelling proceeds, at the expense of the Bragg peak, is observed on planar spectra for the oil and brine dilutions, whereas no significant small-angle signal is seen for the water dilution. Note also that at comparable swelling, the small-angle signal is more intense for the oil dilution than it is for the brine dilution.

Part 2.

In order to describe the scattering properties of lyotropic smectics, we start from the following assumptions : i) the scattering originates in the spatial modulation of the surfactant density $\rho_S(\mathbf{x})$ (the scattering from the (low contrast) solvent is negligible) ; ii) $\rho_S(\mathbf{x})$ is described, at the one-wave level [24], with a wavenumber $q_0 = 2\pi/d$ (d: smectic repeat distance), by :

$$\rho_S(\mathbf{x}) = \bar{\rho} \cdot \{c + \delta c(\mathbf{x})\} + \Delta_S \cos \{q_0 \cdot [z - u(\mathbf{x})]\} \quad (1)$$

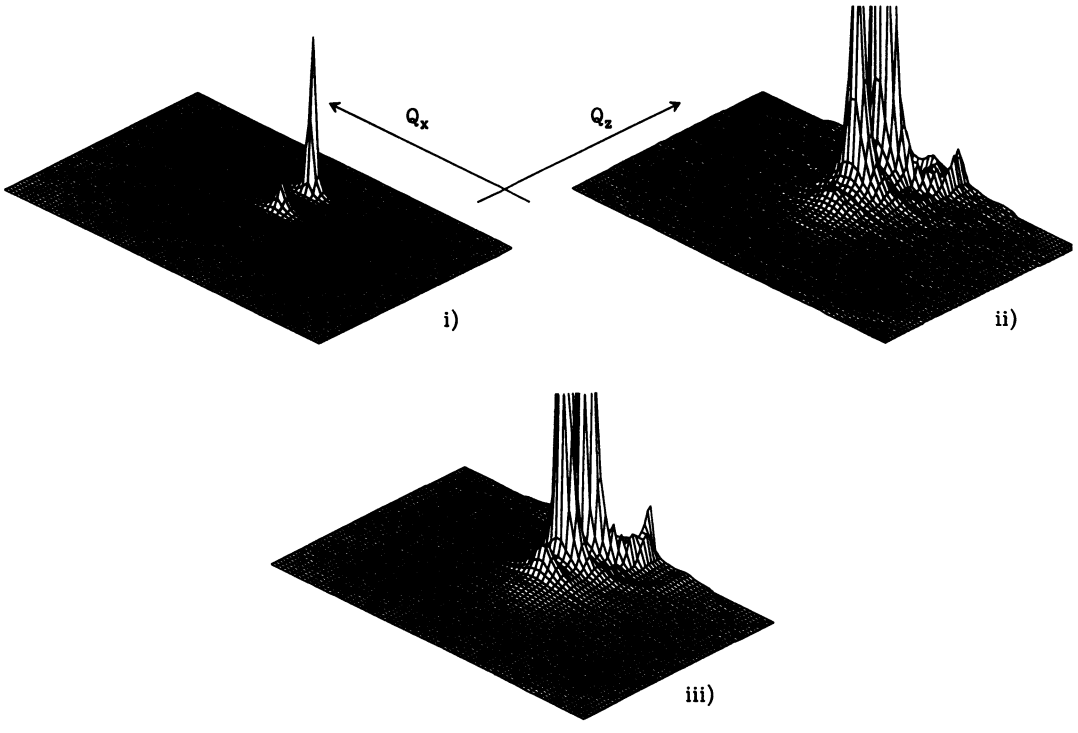

Fig. 3. — Two-dimensional scattering profiles of three water-diluted SDS samples. The smectic repeat distances are, respectively : i) $d = 7.85$ nm ; ii) $d = 9.96$ nm ; iii) $d = 12.2$ nm. The vertical intensity scale has been blown up by a factor ten for graphs ii) and iii) : the third order Bragg peaks are clearly apparent. The low intensity isotropic rings lying on foot of the Bragg peaks arise from unoriented domains.

i.e. we have assumed a perfectly oriented (no defects) and incompressible (non-fluctuating total mass density $\bar{\rho}$) sample, with thermally excited fluctuations in surfactant mass fraction (δc (**x**)) and in layer position (u(**x**)). The amplitude of the modulation, inversely proportional to the smectic repeat distance d, is Δ_S ; it does not fluctuate.

The intensity scattered at a wavevector **q** by an irradiated volume V of such a lyotropic smectic is proportional to :

$$I(\mathbf{q}) = V \int e^{i\mathbf{q}\cdot\mathbf{x}}\, g(\mathbf{x})\, d^3x \tag{2}$$

where the correlation function g is defined as :

$$g(\mathbf{x}) = \frac{|b_S|^2}{m_S^2} \langle \delta\rho_S(\mathbf{0})\, \delta\rho_S(\mathbf{x}) \rangle \ . \tag{3}$$

The surfactant scattering length is b_S, its molecular mass m_S and $\delta\rho$ means : $\rho - \langle \rho \rangle$.

The (Gaussian) fluctuations of concentration δc and layer displacement u are controlled by the harmonic elastic free energy density of a two-component smectic A. We have included gradient terms for the concentration fluctuations, as well as gradient terms for the layer

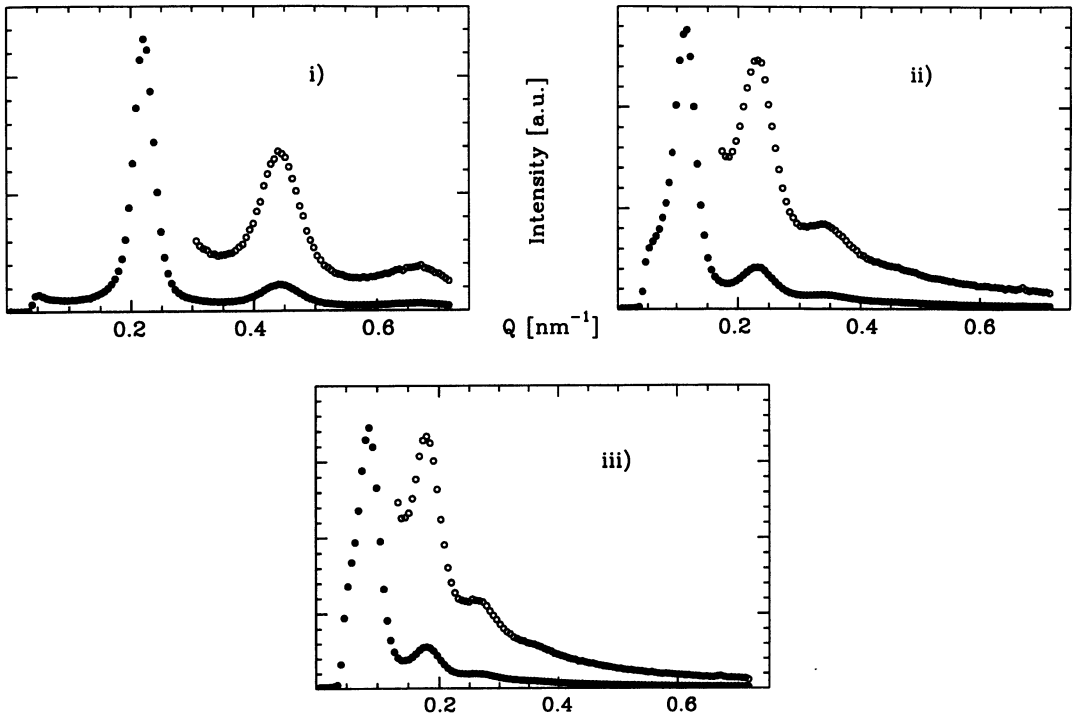

Fig. 4. — One-dimensional scattering profiles of three water-diluted DDAB samples. The smectic repeat distances are, respectively : i) $d = 28.6$ nm ; ii) $d = 57.1$ nm ; iii) $d = 72.4$ nm. For open circles, the vertical intensity scale has been blown up by a factor six. The third order Bragg peak remains at the highest dilutions. There is no significant small-angle scattering.

displacement which are higher order than usual for smectics [25, 26]. These extra terms are required to represent the q-dependence of the (anisotropic) small-angle scattering which appears in the most dilute samples :

$$f = \frac{1}{2}\left\{B(\partial_z u)^2 + K(\nabla_\perp^2 u)^2 + \tilde{K}_1(\partial_{zz}u)^2 + \tilde{K}_2\,\nabla_\perp^2 u\,\partial_{zz}u\right\}$$
$$+ \frac{1}{2\chi}\left\{\delta c^2 + \xi_z^2(\partial_z \delta c)^2 + \xi_\perp^2(\nabla_\perp\,\delta c)^2\right\}$$
$$+ C\,\partial_z u\,\delta c\,. \qquad (4)$$

The elastic constants entering this expression are the usual compression (at constant surfactant concentration) and bending moduli, respectively B and K ; the osmotic compressibility χ ; the lowest order coupling constant C (the compression modulus at constant chemical potential is expressed as : $\bar{B} = B - C^2\chi$) ; and the required higher order (in a wave-vector expansion) terms (the $\tilde{K}$'s) to cope with the concentration gradient terms (ξ_z and $\xi_\perp$ are the correlation lengths for concentration fluctuations respectively along and perpendicular to the layer normal).

The three basic correlation functions derive from the above expression for the free energy density, with the help of the equipartition theorem :

$$\langle u(\mathbf{q})\, u(-\mathbf{q})\rangle = \frac{k_B T}{\bar{B}(\mathbf{q})\, q_z^2 + K q_\perp^4}$$

$$\langle \delta c(\mathbf{q})\, \delta c(-\mathbf{q})\rangle = \frac{k_B T \chi(\mathbf{q})(B(\mathbf{q})\, q_z^2 + K q_\perp^4)}{\bar{B}(\mathbf{q})\, q_z^2 + K q_\perp^4} \tag{5}$$

$$\langle u(\mathbf{q})\, \delta c(-\mathbf{q})\rangle = i \frac{k_B T \chi(\mathbf{q})\, C(\mathbf{q})\, q_z}{\bar{B}(\mathbf{q})\, q_z^2 + K q_\perp^4}.$$

In these expressions, the q-dependent elastic constants are defined as :

$$B(\mathbf{q}) = B + \tilde{K}_1 q_z^2 + \tilde{K}_2 q_\perp^2$$

$$\chi(\mathbf{q}) = \frac{\chi}{1 + \xi_z^2 q_z^2 + \xi_\perp^2 q_\perp^2} \tag{6}$$

$$\bar{B}(\mathbf{q}) = B(\mathbf{q}) - C^2 \chi(\mathbf{q}).$$

The correlation function $g(\mathbf{x})$, related to the intensity of scattered neutrons, can now be evaluated :

$$g(\mathbf{x}) = \left| \frac{b_S \bar{\rho}}{m_S} \right|^2 \langle \delta c(0)\, \delta c(\mathbf{x})\rangle + \frac{1}{2} \left| \frac{b_S \Delta_S}{m_S} \right|^2 \cos(q_0 z) \exp\left(-\frac{q_0^2}{2} \langle (u(\mathbf{x}) - u(0))^2 \rangle \right) \tag{7}$$

In order to obtain this expression, we use the following properties of random Gaussian variables :

$$\langle \cos(X)\rangle = e^{-\frac{\langle X^2\rangle}{2}}$$

$$\langle \sin(X)\, Y\rangle = \langle XY\rangle\, e^{-\frac{\langle X^2\rangle}{2}} \tag{8}$$

and the fundamental Landau-Peierls instability [27, 28] of the one-dimensionaly ordered smectic A phase ($\langle u^2\rangle$ diverges as the logarithm of the size of the system).

The Fourier transform of $g(\mathbf{x})$ gives the intensity scattered by a two-component smectic A. It contains two terms : a low angle part, related to concentration fluctuations, proportional to the function $\langle \delta c(\mathbf{q})\, \delta c(-\mathbf{q})\rangle$ given above ; a quasi-Bragg part, related to the smectic ordering, proportional to the Fourier transform of $\cos(q_0 z) \exp(-q_0^2 \langle (u(\mathbf{x}) - u(\mathbf{0}))^2\rangle /2)$. This last term is essentially the classical [18-20] structure factor of the one-component smectic A, since our expression for the correlation function $\langle u(\mathbf{q})\, u(-\mathbf{q})\rangle$ has the classical long wavelength behaviour. It therefore anisotropically diverges in the vicinity of the Bragg position as :

$$I_B(q_z, \mathbf{q}_\perp = \mathbf{0}) \propto |q_z - q_0|^{-2+\eta}$$

$$I_B(q_z = q_0, \mathbf{q}_\perp) \propto |\mathbf{q}_\perp|^{-4+2\eta} \tag{9}$$

with the exponent η defined in terms of the elastic constants by :

$$\eta = \frac{q_0^2 k_B T}{8\pi \sqrt{K \bar{B}}}. \tag{10}$$

Note that the intensity is scattered *anisotropically,* not only around the Bragg positions, but at small angles too, owing to the anisotropic coupling between layer displacement and concentration fluctuations. This is easily seen in the following zero angle limits :

$$\begin{aligned} \langle \delta c(q_z, 0)\, \delta c(-q_z, 0) \rangle &\to k_B T \frac{\chi B}{\bar{B}}, \quad q_z \to 0 \\ \langle \delta c(0, \mathbf{q}_\perp)\, \delta c(0, -\mathbf{q}_\perp) \rangle &\to k_B T \chi, \quad \mathbf{q}_\perp \to 0 . \end{aligned} \tag{11}$$

The scattering is more intense by a factor $B/\bar{B}$ along q_z, than it is along $q_\perp$ (note that by definition $\bar{B}$ is always smaller than B). The spatial extent of the small-angle scattering is also different along z and $\perp$ axes : in both directions, the functional form is that of an Ornstein-Zernike behaviour, with different compressibilities as already mentioned, and with different effective correlation lengths $\xi_{z\,\mathrm{eff}}$ and $\xi_{\perp\,\mathrm{eff}}$. An expansion of the denominator of the concentration correlation function, respectively in powers of q_z at $q_\perp = 0$ or in powers of $q_\perp$ at $q_z = 0$, yields :

$$\begin{aligned} \xi^2_{z\,\mathrm{eff}} &= \frac{B}{\bar{B}} \left(\xi_z^2 + \frac{\chi C^2}{B} \frac{\tilde{K}_1}{B} \right) \\ \xi^2_{\perp\,\mathrm{eff}} &= \xi_\perp^2 . \end{aligned} \tag{12}$$

Some of the numerous elastic constants that enter the free energy density formula, namely the lowest order ones B, C, χ and K, can be calculated with the help of simple microscopic models of colloidal smectics. We shall here consider the two paradigms of many dilute lamellar phases : rigid surfactant membranes with unscreened electrostatic repulsions between lamellae (electrostatically stabilized lamellar phases) [12, 15, 25] ; flexible surfactant membranes and Helfrich's steric repulsions (sterically stabilized lamellar phases) [8-11, 29]. In the first case, where the membranes are not expected to be significantly crumpled, the main mechanism for surfactant concentration fluctuations at constant smectic repeat distance d is the local variation in the thickness δ of the surfactant membrane (Fig. 5a) ; indeed, on geometrical grounds, the link between concentration (mass fraction) c, thickness δ and spacing d is given by :

$$c = \frac{m_S}{\bar{\rho} v_S} \frac{\delta}{d} \tag{13}$$

(v_S is the surfactant molecular volume).

On the other hand, for sterically stabilized colloidal smectics the surfactant membranes are expected to be crumpled [30-32]. Changes in the crumpling ratio A_B/A (A is the total area of a surfactant membrane, A_B its « base » area, see Fig. 5b) at constant layer spacing become the dominant mechanism for surfactant concentration fluctuations [29]. The swelling law here becomes :

$$c = \frac{m_S}{\bar{\rho} v_S} \frac{A}{A_B} \frac{\delta}{d} \tag{14}$$

where the crumpling ratio involves (experimentally relevant [5]) logarithmic [10, 29, 31] corrections to the simple $1/d$ swelling law.

At a given concentration c, the equilibrium values for d and δ (electrostatically stabilized systems) or for d and A/A_B (sterically stabilized ones) result from two competing effects : repulsive interactions, direct or steric, which favour large repeat distances d; and the

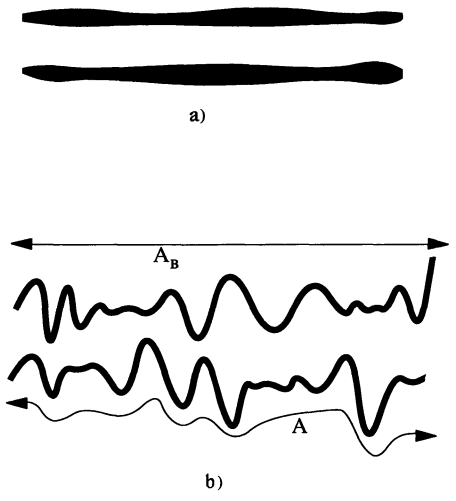

Fig. 5. — Schematic representation of concentration fluctuations at constant layer spacing occurring in lyotropic smectics : a) membrane thickness fluctuations, relevant for flat (rigid) membranes ; b) crumpling ratio fluctuations, relevant for crumpled (flexible) membranes.

selection of an optimum thickness, or crumpling ratio, which prefers a particular value of d for a given concentration. A model for the free energy per unit volume of the stack structure which features this competition is the following sum of two terms :

$$f = \frac{V(d)}{d} + \frac{1}{2} U(X - X_0)^2 . \tag{15}$$

The interaction potential per unit area is $V(d)$; the second term describes in the harmonic approximation, with a characteristic energy per unit volume U, the departure of X (ratio of the membrane thickness to its preferred value, δ/δ_0, or crumpling ratio, A/A_B) from its optimum value X_0 (1 or close to one, up to logarithmic corrections [29]).

For unscreened electrostatic interactions, the interaction potential is [33] :

$$V(d) = \frac{\pi k_B T}{4 L_b d} \tag{16}$$

(L_b is the Bjerrum length of the solvent) and the characteristic energy U can be taken as the product of ε, a characteristic molecular energy presumably of the order of $k_B T$, by the surfactant number density $\bar{\rho} c/m_S$.

For sterically stabilized systems, the interaction potential becomes :

$$V(d) = \frac{3 \pi^2 (k_B T)^2}{128 \kappa d^2} \tag{17}$$

(the numerical constant entering this expression is the one given by Helfrich [8]) and the energy U is given by [29] :

$$U = \frac{12 \pi^2 \kappa}{\left(1 - \frac{4}{\pi^2}\right) d^3} . \tag{18}$$

The elastic constants B, χ^{-1} and C are then obtained by an expansion, up to second order in δd and δc, of the free energy density around an equilibrium state $\{c, d_{eq}(c)\}$; we get :

i) electrostatically stabilized colloidal smectics [15] :

$$\chi^{-1} \approx \frac{\bar{\rho}^2 v_S \varepsilon d}{m_S^2 \delta}, \quad B \approx \frac{\varepsilon \delta}{v_S d}, \quad C \approx \frac{\bar{\rho} \varepsilon}{m_S}$$
$$\bar{B} = \frac{\pi k_B T}{2 L_b d^2} \tag{19}$$

ii) sterically stabilized colloidal smectics [29] :

$$\chi^{-1} \approx \frac{12 \pi^2 v_S^2 \bar{\rho}^2 \kappa}{\left(1 - \frac{4}{\pi^2}\right) m_S^2 \delta^2 d}, \quad B \approx \frac{12 \pi^2 \kappa}{\left(1 - \frac{4}{\pi^2}\right) d^3}, \quad C \approx \frac{12 \pi^2 v_S \bar{\rho} \kappa}{\left(1 - \frac{4}{\pi^2}\right) m_S \delta d^2}$$
$$\bar{B} \approx \frac{9 \pi^2 (k_B T)^2}{64 \kappa d^3}. \tag{20}$$

For both kinds of systems, the smectic splay constant K is related to the membrane bending modulus κ by : $K = \kappa / d$.

The values of the elastic constants can then be used in order to predict some characteristic features of both the Bragg singularities and the small-angle scattering.

i) STERICALLY STABILIZED COLLOIDAL SMECTICS. — In this case, the exponent η is an universal constant [11], $\eta = 4/3$, at large dilution. Since the exponents η_m associated to the m-th order quasi-Bragg peak scale as $m^2 . \eta$ [18, 19], all the η_m for m greater or equal to 2 are larger than 2. Therefore, the Bragg singularities of order two or higher consist in the *vanishing* of the structure factor (as $|q_z - m . q_0|^{-2+\eta_m}$ along q_z, for instance) instead of its divergence : no Bragg peak apart from the first order one is expected for such dilute lamellar phases. The height of the first order Bragg peak (taking into account the finite size of the irradiated sample and the resolution of the experimental set-up), properly normalized, can be shown [19] to scale as $\lambda^{1-\eta}/d^2$, where λ is the smectic penetration length : $\lambda = (K/\bar{B})^{1/2}$. Hence, since a sterically stabilized colloidal smectic has $\lambda = \frac{8}{3\pi} \frac{\kappa}{k_B T} d$, the first order Bragg peak vanishes as $d^{-7/3}$ when the repeat distance d increases.

The osmotic compressibility χ is an increasing function of the repeat distance, $\chi \propto d$, and the ratio $B/\bar{B}$ is large, independent of dilution, proportional to the square of the membrane bending modulus [29] :

$$\frac{B}{\bar{B}} = \frac{256}{3 - \frac{12}{\pi^2}} \left(\frac{\kappa}{k_B T}\right)^2. \tag{21}$$

It results that the small-angle signal is more intense for more dilute samples, therefore overwhelming the Bragg signal : the relative Bragg over small-angle intensity scales as $d^{-10/3}$; the small-angle signal is also very asymmetric and all the more asymmetric as the membranes are less flexible.

ii) ELECTROSTATICALLY STABILIZED COLLOIDAL SMECTICS. — The exponent η is given in this case by :

$$\eta = \sqrt{\frac{\pi k_B T L_b}{2 \kappa d}} . \tag{22}$$

It is asymptotically zero for large repeat distances d : the quasi-Bragg singularities remain power law divergences and more than the first order Bragg peak can be observed. With $\lambda = \sqrt{\frac{2 \kappa L_b d}{\pi k_B T}}$, the height of the Bragg peaks scales as $d^{-3/2}$.

Since the osmotic compressibility χ now decreases when the surfactant concentration is decreased ($\chi \propto c$), the small-angle signal $I(0, \mathbf{q}_\perp)$ has a vanishing intensity at high dilution along the $\perp$ direction ; on the other hand, the product $\chi B/\bar{B}$ is a constant, of the order the osmotic compressibility of any ordinary binary fluid. This means that the small-angle signal $I(q_z, \mathbf{0})$ is weak and does not vary with dilution. Ultimately, the small-angle signal along q_z nevertheless dominates over the Bragg signal since the *relative* Bragg to small-angle intensity goes as $d^{-3/2}$. Nevertheless, that effect is much weaker than in sterically stabilized systems and, except perhaps at very high dilutions, the small-angle scattering will not be a conspicuous feature in the spectrum of dilute, electrostatically stabilized colloidal smectics.

Part 3.

We wish now to compare the model described in the preceding section to our experimental spectra. As already noted in Part 1, our samples are not *perfectly* oriented : the comparison can be at best semi-quantitative. In particular, we shall not attempt to fit the theoretical intensity $I(q_z, \mathbf{q}_\perp)$ to the experimental data. In what follows, we restrict ourselves to one-dimensional fits along the particular direction q_z. Moreover, since the detailed description of the Bragg singularity requires high-resolution spectroscopy [11, 20] which is not attainable with neutrons as probing radiations, we simplify the theoretical description of its shape, using a *Lorentzian* form (Bragg peaks in smectics are not resolution-limited, Eq. (9)). The fitting function along the q_z direction is therefore chosen as :

$$I(q_z, 0) = \frac{A_z}{1 + q_z^2 \xi_{z\,\mathrm{eff}}^2} + \frac{A_B}{(|q_z/q_0| - 1)^2 + R} + B . \tag{23}$$

The fitting parameters are the amplitudes of the small-angle and Bragg scattering, respectively A_z and A_B, the effective correlation length for concentration fluctuations along the z axis, $\xi_{z\,\mathrm{eff}}$, and parameters related to the resolution of the spectrometer, R, and to the background isotropic incoherent scattering, B. The position of the Bragg peak, q_0, is fixed to its measured value, or to its extrapolated value for the most diluted samples. In figure 6 are displayed some representative fits, for the oil-diluted samples. With the fitted parameters from the 1-D spectra, supplemented by reasonable guesses for the other elastic parameters [15, 29], it is possible to reconstruct theoretically the two-dimensional spectrum $I(q_z, \mathbf{q}_\perp)$. Figure 7 illustrates qualitatively the validity of such a procedure.

The relevant parameters extracted from the one-dimensional fits, the effective correlation length along z, $\xi_{z\,\mathrm{eff}}$ and the relative Bragg to small-angle intensity, A_B/RA_z are plotted as functions of the smectic repeat distance d in figure 8. The relative intensity can unfortunately not be extracted from the data at both ends of the dilution line, where either the Bragg or the small-angle intensities are too strong to allow a meaningful fit. The strong decrease of the relative intensity is somewhat slower than the theoretically expected – 10/3 power law. On

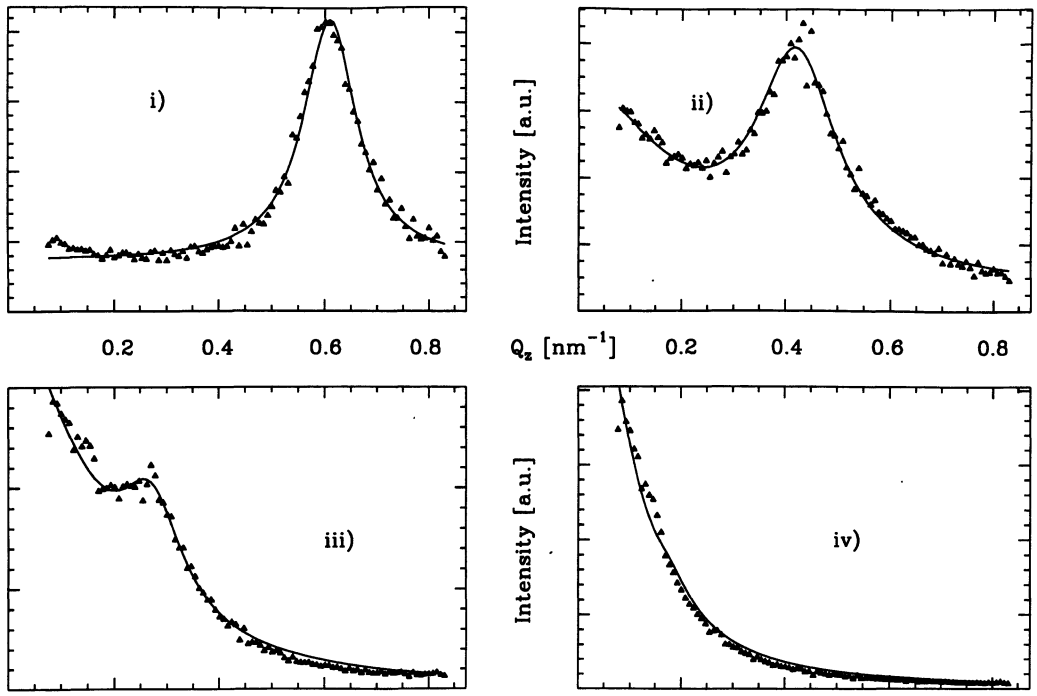

Fig. 6. — Fits of the theoretical lineshape to experimental data (oil-diluted SDS samples), along the q_z axis : i) no significant small-angle scattering ; d = 10.3 nm ; ii) and iii) comparable Bragg and small-angle scattering ; d = 15.0 nm and d = 23.3 nm ; iv) no significant Bragg scattering ; d = 34.9 nm.

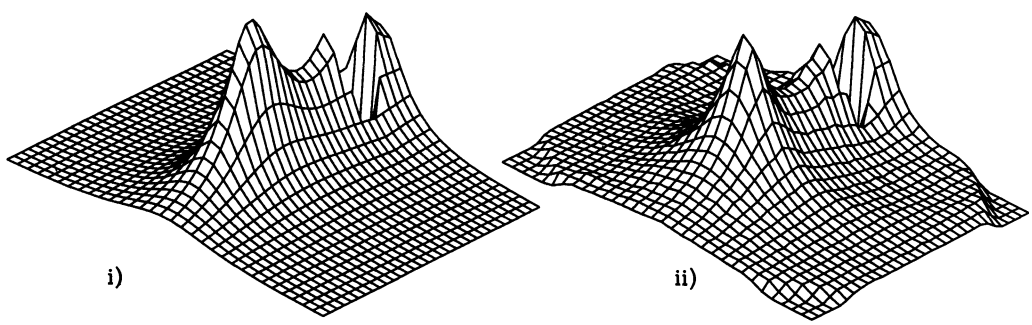

Fig. 7. — Two-dimensional scattering profiles of lyotropic smectics A : i) theoretical profile ; ii) experimental profile. The elastic parameters correspond to an oil-diluted SDS sample with a smectic repeat distance d = 15.0 nm (Fig. 1ii).

the other hand, there is as yet no firm theoretical expectations for the behaviour of $\xi_{z\,\mathrm{eff}}$: it involves the higher order elastic constant $\tilde{K}_1$. If we tentatively assume that $\frac{\tilde{K}_1}{B}$ is close to ξ_z^2, then $\xi_{z\,\mathrm{eff}}$ is enhanced with respect to ξ_z by the large factor $B/\bar{B}$. The observed behaviour is then simply the plausible $\xi_z \propto d$.

For the brine and water-diluted samples, the data are not good enough to allow a sensible

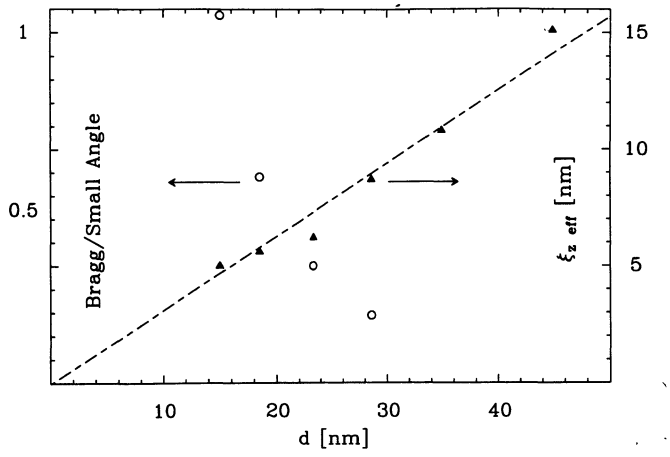

Fig. 8. — Bragg to small-angle relative intensity (open circles, left scale) and effective correlation length $\xi_{z\,eff}$ (filled triangles, right scale), from fits to experimental data on oil-diluted SDS samples. The dotted line is a guide to the eye.

fitting procedure. We simply note qualitative agreement on the following points : the *magnitude* and *asymmetry* of the small-angle scattering are less for the brine-diluted samples than for oil-diluted ones, at comparable dilutions, as expected for more flexible [14] membranes ; the small-angle scattering is very weak for water-diluted samples, as expected for electrostatically interacting membranes.

Conclusion.

The small-angle scattering observed in colloidal smectics is described as arising from the anisotropic coupling between concentration and layer displacement fluctuations. The structure factor is calculated from the most general harmonic form for the elastic free energy of a two-component smectic A phase, taking into account the lowest order gradient terms in concentration fluctuations. Elastic constants can in principle be obtained from a quantitative measurement of the shape of the anisotropic diffusion spectrum. This would presumably require high-resolution X-ray or light scattering, on *perfectly* oriented samples. Our small-angle neutron scattering experiment is in qualitative agreement with the proposed model : for the case of colloidal smectics stabilized by the Helfrich's steric repulsion, the small-angle signal is both more intense and more anisotropic for less flexible membranes ; for electrostatically stabilized systems, there is essentially no small-angle scattering, because of the much smaller values of the relevant compressibilities.

Acknowledgments.

The authors would like to express their gratitude to Tom Lubensky, Sriram Ramaswamy and especially Jacques Prost for numerous and useful discussions, and also for the communication of their preprint. They acknowledge discussions with Grégoire Porte and Cyrus Safinya. They thank Jean Charvolin and Yolande Hendrikx for their assistance in the design of the experimental cells, and Thomas Zemb and Monique Dubois for their gift of the DDAB surfactant.

The hospitality of Laboratoire Léon-Brillouin, with special thanks to Loïc Auvray and Annie Brulet, is gratefully acknowledged.

References

[1] LARCHÉ F., APPELL J., PORTE G., BASSEREAU P. and MARIGNAN J., *Phys. Rev. Lett.* **56** (1986) 1700.

[2] LICHTERFELD F., SCHMELING T. and STREY R., *J. Phys. Chem.* **90** (1986) 5762.

[3] SATOH N. and TSUJII K., *J. Phys. Chem.* **91** (1987) 6629.

[4] IMAE T., SASAKI M. and IKEDA S., *J. Colloid Interface Sci.* **131** (1989) 601.

[5] STREY R., SCHOMÄCKER R., ROUX D., NALLET F. and OLSSON U., *J. Chem. Soc. Faraday Trans.* **86** (1990) 2253.

[6] LENEVEU D., RAND R. P. and PARSEGIAN V. A., *Nature* **259** (1976) 601.

[7] HELFRICH W., *Phys. Lett.* **A 43** (1973) 409.

[8] HELFRICH W., *Z. Naturforsch.* **33a** (1978) 305.

[9] LEIBLER S. and LIPOWSKY R., *Phys. Rev.* **B35** (1987) 7004.

[10] GOLUBOVIČ L. and LUBENSKY T. C., *Phys. Rev.* **B39** (1989) 12110.

[11] SAFINYA C. R., ROUX D., SMITH G. S., SINHA S. K., DIMON P., CLARK N. A. and BELLOCQ A.-M., *Phys. Rev. Lett.* **57** (1986) 2718.

[12] ROUX D. and SAFINYA C. R., *J. Phys. France* **49** (1988) 307.

[13] SAFINYA C. R., SIROTA E. B., ROUX D. and SMITH G. S., *Phys. Rev. Lett.* **62** (1989) 1134.

[14] NALLET F., ROUX D. and PROST J., *Phys. Rev. Lett.* **62** (1989) 276.

[15] NALLET F., ROUX D. and PROST J., *J. Phys. France* **50** (1989) 3147.

[16] RICHETTI P., KÉKICHEFF P., PARKER J. L. and NINHAM B. W., *Nature* **346** (1990) 252.

[17] BASSEREAU P., MARIGNAN J. and PORTE G., *J. Phys. France* **48** (1987) 673.

[18] CAILLÉ A., *C. R. Hebdo. Acad. Sci. Paris* **B 274** (1972) 891.

[19] GUNTHER L., IMRY Y. and LAJZEROWICZ J., *Phys. Rev.* **A 22** (1980) 1733.

[20] ALS-NIELSEN J., LITSTER J. D., BIRGENEAU R. J., KAPLAN M., SAFINYA C. R., LINDEGAARD-ANDERSEN A. and MATHIESEN S., *Phys. Rev.* **B 22** (1980) 312.

[21] PORTE G., BASSEREAU P., MARIGNAN J. and MAY R., Physics of Amphiphilic Layers, Meunier, Langevin and Boccara Eds. (Springer Verlag) 1987.

[22] PORTE G., MARIGNAN J., BASSEREAU P. and MAY R., *Europhys. Lett.* **7** (1988) 713.

[23] CHARVOLIN J. and HENDRIKX Y., private communication.

[24] DE GENNES P.-G., *Solid State Commun.* **10** (1972) 753.

[25] BROCHARD F. and DE GENNES P.-G., *Pramana Suppl.* **1** (1975) 1.

[26] GRINSTEIN G. and PELCOVITS R. A., *Phys. Rev.* **A 26** (1982) 915.

[27] PEIERLS R. E., *Proc. Cambridge Philos. Soc.* **32** (1934) 477.

[28] LANDAU L. D., *Phys. Z. Sowjetunion* **11** (1937) 26.

[29] LUBENSKY T. C., PROST J. and RAMASWAMY S., *J. Phys. France* **51** (1990) 933.

[30] DE GENNES P.-G. and TAUPIN C., *J. Phys. Chem.* **86** (1982) 2294.

[31] HELFRICH W. and SERVUSS R.-M., *Nuovo Cimento* **D 3** (1984) 137.

[32] PELITI L. and LEIBLER S., *Phys. Rev. Lett.* **54** (1985) 1690.

[33] COWLEY A. C., FULLER N. L., RAND R. P. and PARSEGIAN V. A., *Biochemistry* **17** (1978) 3163.